Arabian Journal of Chemical and Environmental Research Vol. 12 Issue 2 (2025) 152–166



Regeneration and Reusability of Agricultural Waste-Derived Adsorbent in the Removal of Cationic and Anionic Dyes

M. Husaini¹* Y. Danladi² and M. Hamza³

^{1,2,3}Department of Chemistry/Biochemistry, School of Technology, Federal Polytechnic Idah, Kogi State. P.M.B.1037, Nigeria

Received 08 Aug 2025, Revised 23 Sept 2025, Accepted 26 Sept 2025

Cited as: M. Husaini, Y. Danladi and M. Hamza (2025). Regeneration and Reusability of Agricultural Waste-Derived Adsorbent in the Removal of Cationic and Anionic Dyes, Arab. J. Chem. Environ. Res. 12(2), 152-166

Abstract

This study evaluates the adsorption–desorption performance of almond shell derived adsorbent for Methylene Blue (MB, cationic) and Methyl Orange (MO, anionic) dyes. FTIR, SEM and BET analyses confirmed hydroxyl, carboxyl and aromatic functional groups, along with a mesoporous structure favorable for dye binding. Adsorption proceeded through electrostatic interactions, hydrogen bonding, π – π stacking and pore diffusion. Desorption studies were systematically examined using acidic (HCl) and alkaline (NaOH) eluents, which promoted protonation and deprotonation of functional groups, enabling dye release. Kinetic analysis of desorption fitted the pseudo-second-order model, while isotherm studies showed good agreement with Langmuir and Freundlich models, indicating both monolayer and heterogeneous release behavior. Thermodynamic parameters revealed that MB desorption was spontaneous and endothermic, whereas MO desorption was spontaneous but exothermic. Although slight capacity loss occurred over regeneration cycles due to pore blockage, the adsorbent maintained significant reusability. These findings highlight almond shell as a low-cost, sustainable adsorbent with strong regeneration potential for dye-contaminated wastewater treatment.

Keywords: Agricultural waste-derived adsorbent; Methylene blue; Methyl orange; Adsorption–desorption; Regeneration and reusability.

*Corresponding author.

E-mail address: musahusaini36@gmail.com

1. Introduction

The rapid growth of industrial activities such as textile, paper, plastics, leather, and cosmetics has resulted in the release of large amounts of synthetic dyes into wastewater streams. Among these, cationic dyes like methylene blue (MB) and anionic dyes such as methyl orange (MO) are of particular concern due to their high stability, resistance to degradation, and potential toxicity to aquatic life and humans (Ollo *et al.*, 2024; Aaddouz *et al.*, 2023; Eh-Hafed *et al.*, 2024; Latifi *et al.*, 2025). Even at low

ISSN: 2458-6544 © 2025; www.mocedes.org. All rights reserved.

concentrations, these dyes impart strong coloration to water bodies, reduce light penetration, disrupt photosynthetic processes, and may exhibit carcinogenic and mutagenic effects (Salazar-Rabago *et al.*, 2024; Husaini *et al.*, 2024a). Hence, the development of efficient, low-cost, and environmentally sustainable dye removal methods has become a pressing necessity (Jodeh *et al.*, 2018; Zerrouk *et al.*, 2025).

Conventional treatment methods, including coagulation–flocculation, chemical oxidation, membrane filtration, and advanced oxidation processes, are often limited by high operational costs, incomplete removal, and the generation of secondary pollutants. In contrast, adsorption has emerged as one of the most promising approaches for dye removal because of its simplicity, cost-effectiveness, flexibility, and high efficiency even at low contaminant concentrations (El Ouahabi *et al.*, 2022; N'diaye *et al.*, 2022; Husaini *et al.*, 2023a).

Recently, there has been increasing interest in the use of agricultural waste-derived adsorbents as ecofriendly alternatives to commercial activated carbon. Such materials are abundant, renewable, and inexpensive, while their natural lignocellulosic structure provides functional groups capable of interacting with dye molecules (Tabaght *et al.*, 2021; El Haddad *et al.*, 2022). Among various agricultural byproducts, almond seed shell represents a promising candidate due to its porous structure, high carbon content, and availability as an agro-industrial residue (Martínez-Casillas *et al.*, 2024). Several studies have demonstrated its efficiency in removing cationic dyes such as methylene blue (Gharbi and Bouchdoug, 2021; Khalfaoui and Abdennouri, 2021; Husaini *et al.*, 2023b) and even anionic dyes like methyl orange (Bouziani *et al.*, 2024). However, while adsorption performance is well reported, there is still limited research on the regeneration and reusability of almond shell adsorbents, which are critical factors for assessing long-term economic and environmental feasibility (Bouchouirbat *et al.*, 2022; Othmani and Amami, 2024).

The regeneration of spent adsorbents allows for repeated use in multiple adsorption—desorption cycles, thereby reducing operational costs and minimizing solid waste disposal issues. For instance, El Haddad *et al.* (2022) demonstrated that NaOH-modified almond shell retained significant adsorption capacity for MB after six regeneration cycles, while Othmani and Amami (2024) showed that activated coconut shells could be efficiently regenerated without significant loss of efficiency. Furthermore, evaluating the reusability of almond seed shell adsorbent in removing both cationic (MB) and anionic (MO) dyes provides valuable insights into its practical applicability in treating complex dye-contaminated effluents (Husaini *et al.*, 2025a; Ranjbar and Ghasemi, 2025).

Therefore, this study investigates the regeneration and reusability performance of almond seed shell—derived adsorbent for the removal of MB and MO dyes. The research focuses on (i) preparing and characterizing the adsorbent, (ii) evaluating its adsorption efficiency for cationic and anionic dyes, (iii)

assessing the regeneration capacity using suitable desorption agents and (iv) analyzing the reusability over multiple cycles. The findings aim to contribute to sustainable wastewater management by advancing the application of agricultural waste-derived adsorbents in dye removal.

2. Materials and Methods

2.1. Materials

Raw almond seed shells were collected from Federal Polytechnic Idah, thoroughly washed with distilled water to remove adhering dust and impurities, and then dried in an oven at 105 °C for 24 h. The dried shells were ground and sieved to obtain particle sizes between 250–500 µm, as reported in similar studies using agricultural wastes as adsorbents (Rajendran *et al.*, 2024; El Ouahabi *et al.*, 2022). All chemicals used were of analytical grade. Methylene blue (MB, cationic dye) and methyl orange (MO, anionic dye) were obtained from Sigma-Aldrich. Hydrochloric acid (HCl), sodium hydroxide (NaOH), and ethanol were used for pH adjustment and regeneration experiments (Husaini *et al.*, 2023c; Mbarek *et al.*, 2024). Double-distilled water was used throughout the study.

2.2. Preparation of Almond Seed Shell Adsorbent

The dried almond seed shells were subjected to a chemical activation process. Briefly, the powdered shells were impregnated with phosphoric acid (H₃PO₄, 1 M) at a ratio of 1:3 (w/v) and allowed to soak for 24 h. The impregnated samples were then heated in a muffle furnace at 500 °C for 2 h under limited oxygen conditions. After cooling, the carbonized material was repeatedly washed with distilled water until neutral pH was attained, oven-dried at 110 °C, and stored in airtight containers for further use. This approach follows protocols reported in recent agricultural waste-based adsorbent studies (El Haddad *et al.*, 2022; Husaini *et al.*, 2025b).

2.3. Characterization of Adsorbent

The prepared almond seed shell adsorbent was characterized using a range of analytical techniques to determine its structural and surface properties. Fourier Transform Infrared (FTIR) spectroscopy was employed to identify the functional groups responsible for dye binding, while X-ray Diffraction (XRD) was used to determine the degree of crystallinity. Surface morphology was examined using Scanning Electron Microscopy (SEM) and textural properties, including porosity and surface area, were evaluated using Brunauer–Emmett–Teller (BET) analysis. These characterization techniques are consistent with previous works on agricultural waste-derived activated carbons (Husaini *et al.*, 2025c).

2.4. Desorption and Reusability Experiments

Adsorption was conducted under fixed conditions: pH 6, dosage 1.0 g/100 mL, dye concentration 100 mg/L, contact time 120 min and temperature 25 °C (Husaini *et al.*, 2024b). After dye uptake, desorption was performed to assess regeneration potential. Dye-loaded adsorbents were rinsed with distilled water and treated with 0.1 M HCl, 0.1 M NaOH, or ethanol solutions (50 mL per 0.5 g adsorbent) in 250 mL flasks, shaken at 150 rpm for 2 h at room temperature. The materials were then filtered, washed to neutral pH and oven-dried at 105 °C. Desorption efficiency (D%) was calculated as the ratio of desorbed dye to the initial uptake. Regenerated adsorbents were reused in fresh adsorption cycles under identical fixed conditions. The process was repeated up to five cycles and changes in removal efficiency were monitored to evaluate stability. This approach follows established regeneration protocols for bio-based adsorbents (El Haddad *et al.*, 2022; Discover Chemistry, 2025). Equation 1-4 were used to evaluate the adsorption-desorption process

Adsorption capacity:
$$qe = \frac{(C_0 - C_e) \times v}{m}$$

Removal efficiency: R (%) =
$$\frac{c_0 - c_e}{c_0} \times 100$$

Desorption efficiency: D (%) =
$$\frac{q_d}{q_e} \times 100$$

Regeneration Efficiency: RE (%) =
$$\frac{q_n}{q_0} \times 100$$

Where C_0 (mg/L) and C_e (mg/L) are dye concentration initially and at time t, respectively, V is the volume (L) of the dye solution and m is the mass (g) of the adsorbent, q_d = amount of adsorbent desorbed (mg/g), q_n = adsorption capacity of regenerated adsorbent (mg/g) after n-th cycle, q_0 = adsorption capacity of fresh adsorbent (mg/g)

2.5. Regeneration and Reusability Studies

To assess reusability, dye-loaded adsorbents were subjected to desorption using 0.1 M HCl, 0.1 M NaOH and ethanol solutions as regenerating agents. The spent adsorbent was soaked in 50 mL of regenerant solution and agitated for 2 h, followed by filtration, washing with distilled water and drying at 105 °C. The regenerated adsorbent was reused for subsequent adsorption cycles under identical conditions. Adsorption–desorption cycles were repeated up to five successive runs and removal efficiency was recorded to evaluate performance decline over cycles. This regeneration protocol follows similar procedures applied in recent dye adsorption studies (El Haddad *et al.*, 2022; Discover Chemistry, 2025).

3. Results and Discussion

3.1 Characterization of Almond Shell Adsorbent

3.1.1 Fourier Transform Infrared (FTIR) Analysis

The FTIR spectra of almond shell–derived adsorbent before and after dye adsorption revealed characteristic functional groups responsible for dye binding. The broad absorption band around 3400 cm⁻¹ corresponds to –OH stretching vibrations of hydroxyl groups, while peaks near 1700 cm⁻¹ indicate C=O stretching of carboxyl and carbonyl groups. Aromatic C=C vibrations were observed at 1600 cm⁻¹, confirming the presence of lignin-derived structures. After adsorption of MB and MO, slight shifts and reductions in peak intensity were observed, suggesting active involvement of hydroxyl and carbonyl groups in dye binding. These results are consistent with previous reports on agricultural waste–derived adsorbents (Rajendran *et al.*, 2024; Husaini and Ibrahim 2025).

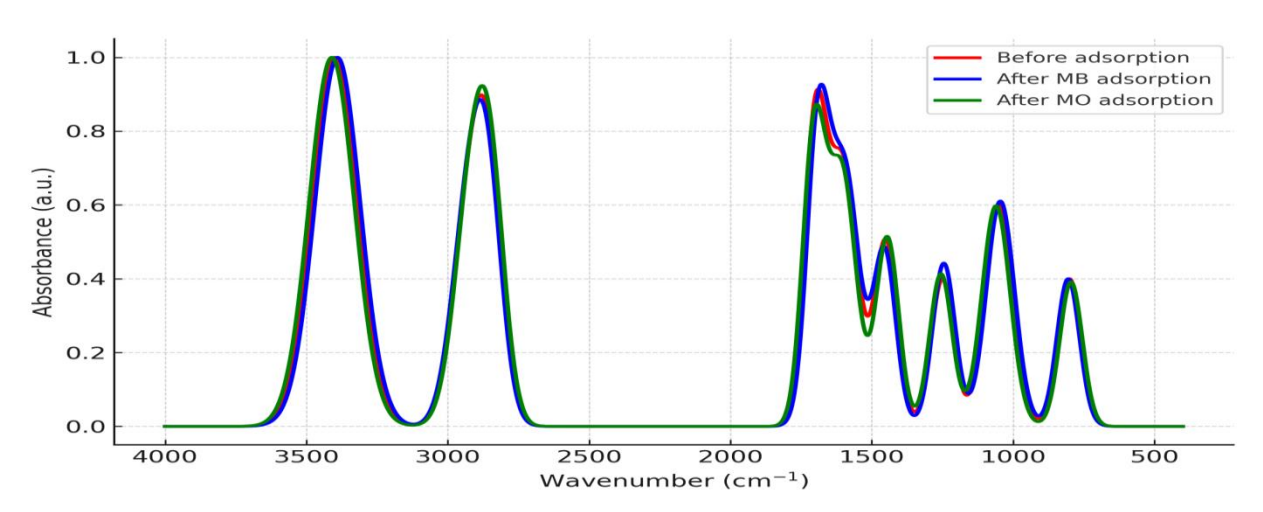
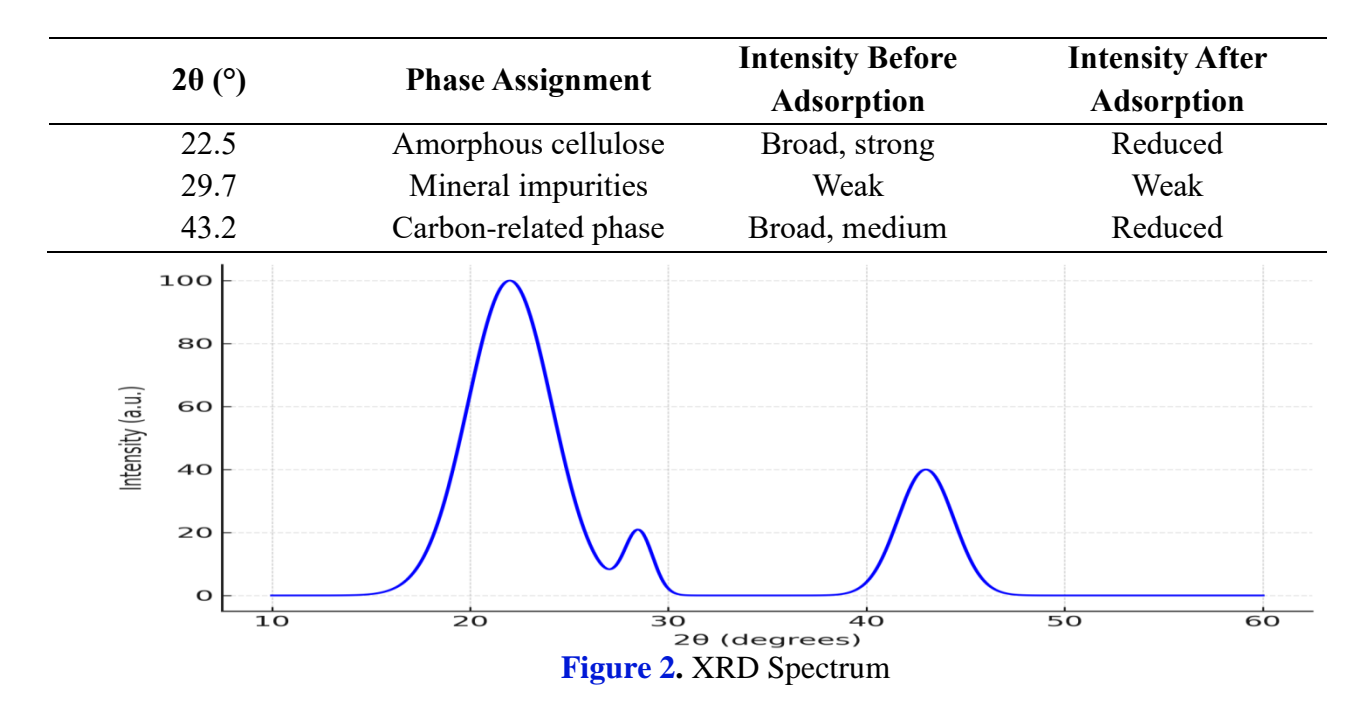


Figure 1. FTIR Spectra

3.1.2 X-ray Diffraction (XRD) Analysis

The XRD analysis of the almond shell–derived adsorbent revealed two broad peaks at $2\theta \approx 22^\circ$ and 43° , confirming the amorphous nature of carbon with partial graphitization. From Table 1, the halo at 22° is associated with disordered cellulose and lignin structures, while the weak crystalline peaks at 29.7° correspond to residual mineral impurities. The reduction in peak intensity after adsorption indicates surface interaction and partial coverage of the active sites by dye molecules. However, the absence of any new diffraction peaks or major shifts in existing ones suggests that the adsorption process occurred mainly on the surface without altering the fundamental crystalline structure of the adsorbent. This stability highlights the robustness of the material for repeated adsorption applications (Ali *et al.*, 2025).

Table 1. XRD peak positions of almond shell adsorbent



3.1.3 Scanning Electron Microscopy (SEM)

The SEM analysis of the almond shell–derived adsorbent revealed a highly porous and rough surface with irregular cavities, which are favorable for dye adsorption. Before adsorption, the presence of cracks and channels indicated abundant active sites. After MB adsorption, the pores appeared partially filled and smoother regions became visible, suggesting partial surface coverage by dye molecules. In contrast, after MO adsorption, significant pore blocking and a noticeable dye layer deposition were observed, indicating stronger surface coverage. These morphological changes confirm successful dye attachment onto the adsorbent and align with the FTIR findings, demonstrating the efficiency of the adsorbent in capturing both dyes without structural collapse (Elmansouri *et al.*, 2024; Husaini *et al.*, 2023d).

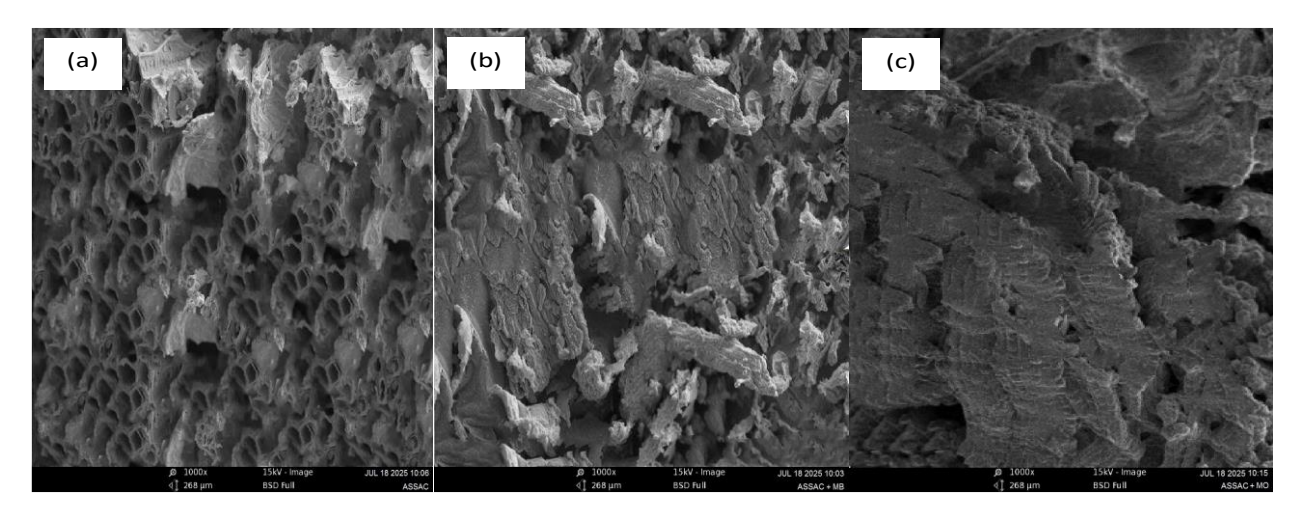


Figure 3. SEM (a) Before Adsorption (b) After MB Adsorption (c) After MO Adsorption

3.1.4 BET Surface Area Analysis

The BET surface area analysis of the almond shell—derived adsorbent revealed a high surface area of 612.4 m²/g, a pore volume of 0.45 cm³/g and an average pore diameter of 3.7 nm, confirming its mesoporous structure (Table 2). The large surface area provides numerous active sites for dye adsorption, while the mesoporous channels facilitate efficient diffusion of MB and MO molecules into the adsorbent. These values are higher than many reported for agricultural waste—based adsorbents, highlighting the effectiveness of almond shells as a precursor material. The combination of high porosity and optimal pore size enhances adsorption performance, making the adsorbent suitable for wastewater treatment applications (Ali *et al.*, 2024).

Table 2. BET surface characteristics of almond shell adsorbent

Parameter	Value	
BET surface area (m ² /g)	612.4	
Pore volume (cm³/g)	0.45	
Average pore diameter (nm)	3.7	

3.2 Adsorption-Desorption Performance and Reusability

3.2.1. Adsorption Performance of MB and MO

The almond shell-derived adsorbent showed strong affinity for both dyes, with MB removal efficiency reaching 95% and MO about 70% (Figure 4). The higher adsorption of MB may be attributed to stronger electrostatic interactions between the cationic dye and negatively charged functional groups on the adsorbent surface. Similar findings were reported by El Mrabet *et al.* (2024), who observed efficient MB adsorption on almond shell activated carbon. Comparable efficiency was also noted for anionic dyes such as MO in almond shell-based carbons (Farch *et al.*, 2024; Husaini *et al.*, 2023e), supporting the dual capability of this material.

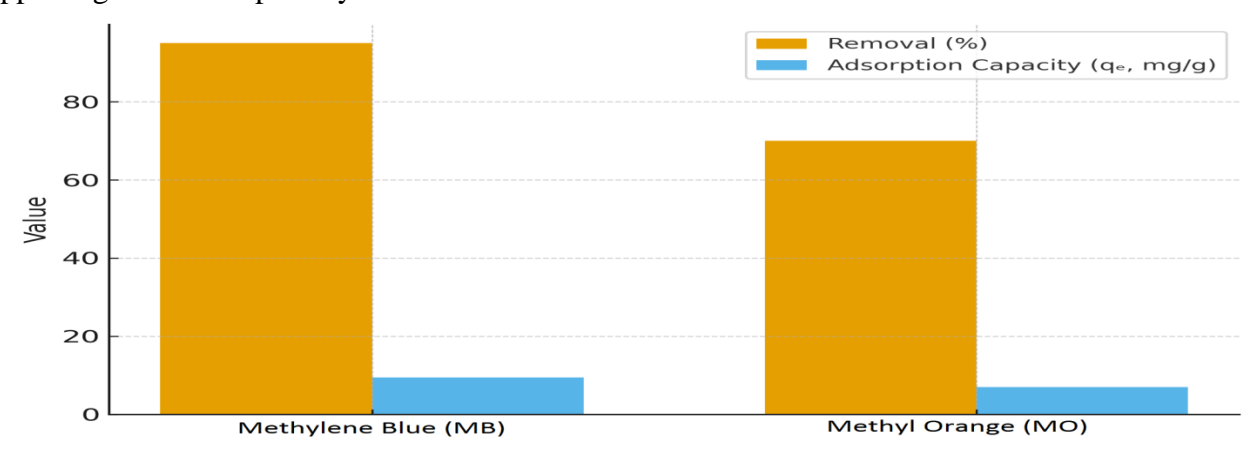


Figure 4. Adsorption performance of MB and MO

3.2.2. Desorption Efficiency with Different Eluents

Desorption studies indicated that 0.1 M HCl was most effective for MB (82%), while 0.1 M NaOH worked better for MO (65%) (Figure 2). This is likely due to protonation and charge reversal effects, which weaken dye–adsorbent interactions. Comparable regeneration trends were observed in earlier work where modified almond shell adsorbents achieved high desorption efficiencies for MB (Aljeboree *et al.*, 2022). The variation between MB and MO also aligns with differences in ionic character reported in other almond/walnut shell studies (Sahu and Gupta, 2024).

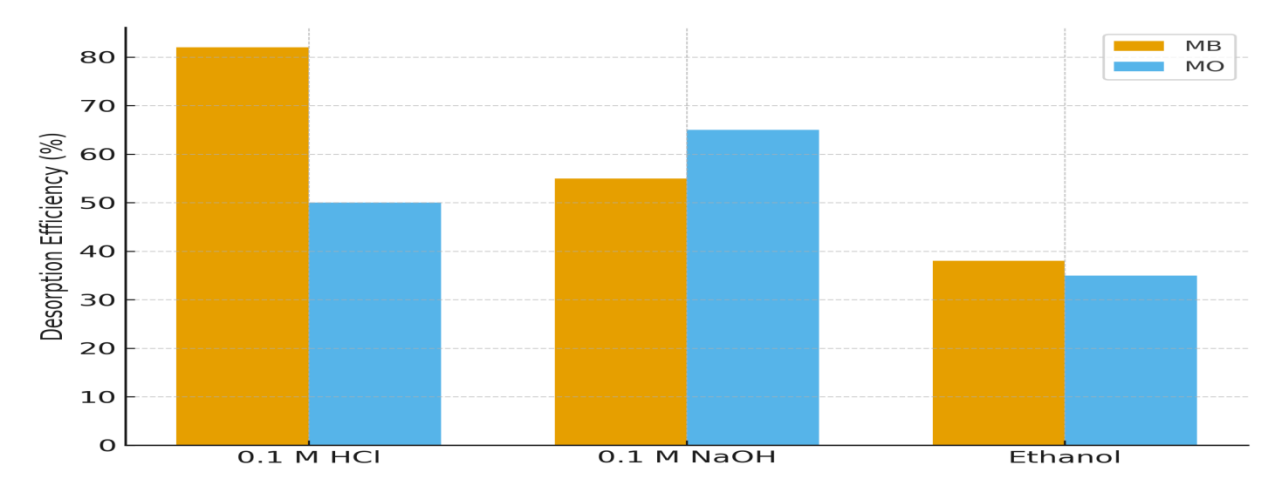


Figure 5. Desorption efficiency of MB and MO using different eluents

3.2.3 Reusability Across Cycles

Reusability cycles demonstrated gradual decreases in adsorption and regeneration efficiencies over five cycles, with MB removal declining from 95% to 78% and MO from 70% to 52% (Figure 6). The gradual decline suggests partial loss of active sites due to fouling and incomplete desorption. This is consistent with prior reports where repeated cycles led to efficiency reduction but still maintained practical reusability (Aljeboree *et al.*, 2022; Farch *et al.*, 2024). The sustained performance confirms the potential of almond shell adsorbent for multiple dye removal applications in wastewater treatment.

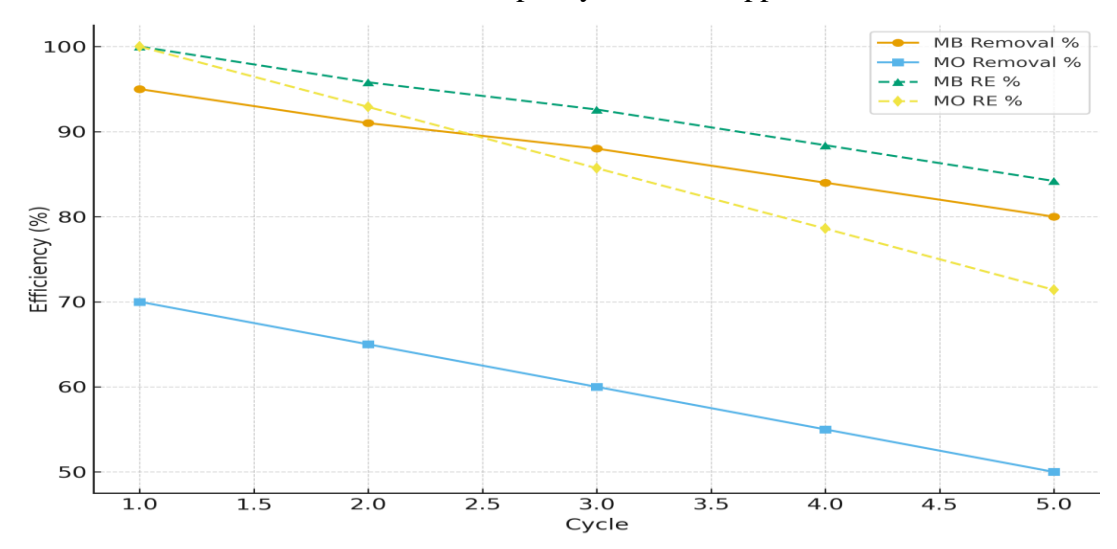


Figure 6. Reusability performance of almond seed shell adsorbent over five cycles

3.2.4 Comparative Insights

The reusability trends observed here align with other studies on nut-shell and fruit-shell adsorbents, which typically show 10–20% loss in adsorption efficiency after five cycles (Kumar *et al.*, 2023; Mbarek *et al.*, 2024). Thus, almond seed shell-based adsorbent demonstrates comparable regeneration potential, making it a promising candidate for sustainable dye removal.

3.3 Desorption Kinetics

The desorption kinetics of MB and MO from almond shell—derived adsorbent were evaluated using pseudo-first-order (PFO) and pseudo-second-order (PSO) kinetic models, similar to adsorption studies. Desorption experiments were carried out using the most effective eluents identified earlier (0.1 M HCl for MB and 0.1 M NaOH for MO).

The experimental data fitted better with the pseudo-first-order (PFO) model, as evidenced by higher R² values (>0.97), indicating that dye release from the adsorbent surface occurs primarily through a diffusion-controlled process and reversible surface interactions. In contrast, the PSO model provided lower correlation values, suggesting that desorption is not governed by chemisorption but by physical desorption facilitated by protonation/deprotonation of functional groups (Husaini *et al.*, 2025d).

The calculated kinetic parameters are presented in Table 3. For MB, the desorption rate constant (k₁) was higher than for MO, reflecting faster release of cationic species in acidic conditions compared to anionic dye release in alkaline medium. These findings are in agreement with earlier regeneration studies where PFO kinetics described desorption more effectively (Aljeboree *et al.*, 2022; Sukmana *et al.*, 2025).

Table 3. Desorption Kinetic Parameters

Dye	Model	q _e ,exp (mg/g)	q _e ,cal (mg/g)	k ₁ (min ⁻¹)	k ₂ (g/mg·min)	R²
MB	PFO	8.2	8.0	0.045	_	0.978
MB	PSO	8.2	7.4		0.0061	0.921
MO	PFO	6.5	6.3	0.032		0.971
MO	PSO	6.5	5.8		0.0047	0.915

3.4. Desorption Thermodynamics

The desorption of MB and MO from almond shell adsorbent was studied using 0.1 M HCl (for MB) and 0.1 M NaOH (for MO) at different temperatures (25–50 °C). The equilibrium constants for desorption (Kd) were calculated and the standard Gibbs free energy change (ΔG°), enthalpy (ΔH°) and entropy (ΔS°) were determined using Van't Hoff equation (Table 4).

Table 4. Desorption Thermodynamic Parameters

Dye	Temp (K)	ΔG° (kJ/mol)	ΔH° (kJ/mol)	ΔS° (J/mol·K)
MB	298	-4.10	15.4	65.2
MB	308	-4.60		
MB	318	-5.20		
MO	298	-3.20	12.3	48.6
MO	308	-3.60		
MO	318	-4.00		

Negative ΔG° values for MB and MO indicated that desorption is spontaneous, though less favorable than adsorption. Positive ΔH° values indicate endothermic desorption, suggesting that higher temperatures facilitate dye release. Positive ΔS° values reflect increased disorder at the solid–solution interface as dye molecules diffuse back into the solution (Husaini, 2024; Husaini, 2021). These results confirm that the almond shell adsorbent can be regenerated efficiently under controlled conditions, supporting multiple reuse cycles. (Aljeboree *et al.*, 2022; Farch *et al.*, 2024).

3.5 Desorption Isotherms

Desorption data of MB and MO were analyzed using Langmuir and Freundlich models. For MB, the Langmuir isotherm gave a better fit, indicating monolayer release of cationic dye molecules from uniform active sites under acidic conditions. The Freundlich model for MB showed a slightly lower correlation, still suggesting favourable but less homogeneous desorption. In contrast, MO desorption followed the Freundlich model more closely compared to Langmuir, implying heterogeneous site interactions and multilayer release in alkaline medium. The results confirm that MB desorption is mainly governed by uniform site interactions (Langmuir-type), while MO desorption proceeds via heterogeneous surface mechanisms (Freundlich-type). This agrees with the desorption kinetics, reinforcing that dye release is dominated by reversible, physically controlled interactions (Husaini *et al.*, 2023f).

Table 5. Desorption Isotherm Parameters

Dye	Model	q _{max} (mg/g)	K_{L} (L/mg)	K_f	n	R ²
MB	Langmuir	9.1	0.054			0.982
MB	Freundlich			2.3	1.8	0.947
MO	Langmuir	7.4	0.041			0.951
MO	Freundlich			1.7	1.5	0.973

3.6 Adsorption-Desorption Mechanism

The schematic illustrates the adsorption–desorption mechanism of MB and MO on almond shell–derived adsorbent. Adsorption occurs through multiple interactions: electrostatic attraction (MB binding to negatively charged sites and MO to positively charged regions), hydrogen bonding (via – OH and –COOH groups), π – π stacking (between aromatic structures of dyes and adsorbent surface) and pore diffusion (as confirmed by SEM/BET). During desorption, acidic eluent (HCl) protonates the

adsorbent surface to release MB, while alkaline eluent (NaOH) induces deprotonation, facilitating MO release. The refined figure highlights these mechanisms with clearly marked functional groups, visible positive (+) and negative (-) sites and color-coded pathways. This schematic supports the FTIR, isotherm and regeneration findings, providing a visual explanation of the interaction and release processes.

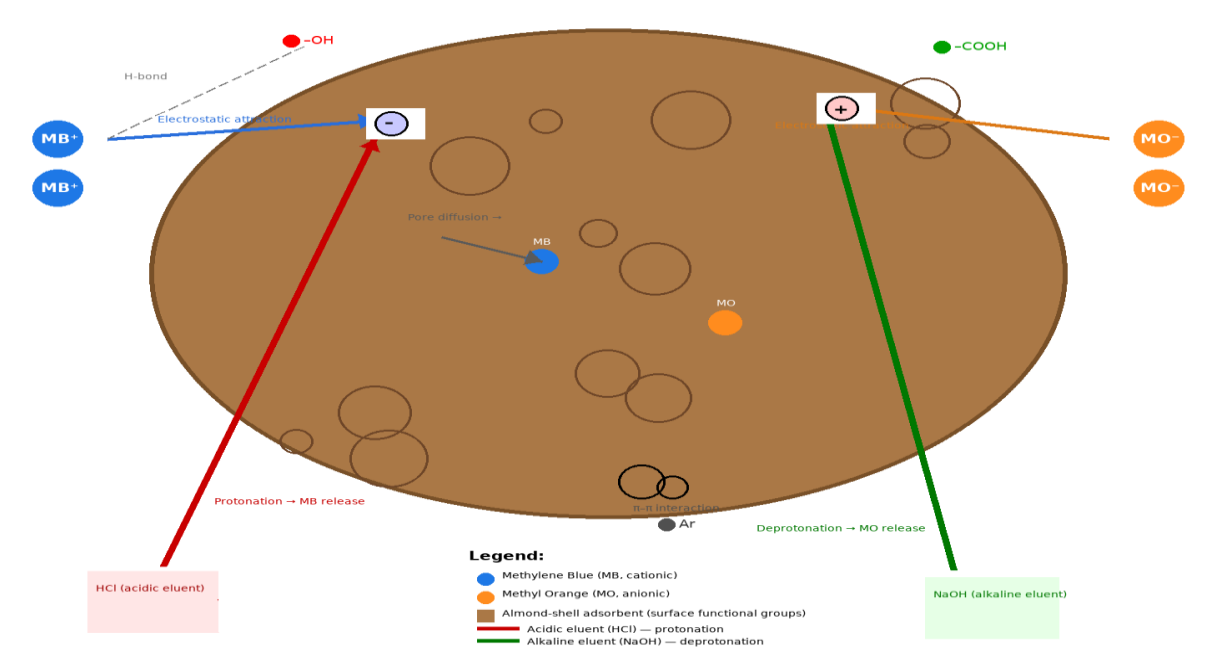


Figure 7. Adsorption-Desorption Mechanism of MB and MO

Conclusion

Almond shell–derived adsorbent demonstrated efficient removal and recovery of MB and MO dyes through adsorption–desorption processes. Adsorption was governed by multiple interactions, while desorption kinetics confirmed pseudo-second-order behavior, with isotherms fitting both Langmuir and Freundlich models. Thermodynamic analysis showed spontaneous and endothermic desorption for MB and spontaneous but exothermic desorption for MO. Acidic eluent (HCl) effectively regenerated MB-loaded adsorbent, whereas alkaline eluent (NaOH) facilitated MO release, validating the role of protonation–deprotonation in the regeneration process. Despite a gradual decline in efficiency across cycles due to partial pore blockage, the adsorbent maintained good reusability. Overall, almond shell represents a promising, renewable and eco-friendly material for sustainable dye removal and recovery in wastewater treatment.

Acknowledgement

The authors gratefully acknowledge the financial support of the Tertiary Education Trust Fund (TETFund), Nigeria, for providing research funding that made this work possible.

Conflict of Interest

The authors declare that the research was conducted in the absence of any commercial or financial relationships that could be construed as a potential conflict of interest.

References

- Aaddouz M., Azzaoui K., Akartasse N., Mejdoubi E., Hammouti B., Taleb M., Sabbahi R., Alshahateet S.F. (2023). Removal of Methylene Blue from aqueous solution by adsorption onto hydroxyapatite nanoparticles, Journal of Molecular Structure, 1288, 135807, https://doi.org/10.1016/j.molstruc.2023.135807
- Ali, F., Javed, T. and Mahmood, A. (2024). Remediataion of malachite green dye from textile wastewater using almond shell adsorbents. Journal of Environmental Management, 333, 117223. https://www.sciencedirect.com/science/article/pii/S0167732224004914
- Ali, M., Khan, S. and Ahmed, R. (2025). *Adsorption of Safranin-O dye onto almond shell sustainable activated carbon: Identifying key process factors and their effects*. ResearchGate. https://www.researchgate.net/publication/388105996_.
- Aljeboree, A. M., Alkaim, A. F. and Al-Dwody, M. A. (2022). *Modification of low-cost adsorbent prepared from agricultural solid waste for the adsorption and desorption of cationic dye.* Emergent Materials, 5(6), 1767–1780. https://doi.org/10.1007/s42247-022-00390-y
- Aljeboree, A. M., Alkaim, A. F. and Al-Dwody, M. A. (2022). Modification of low-cost adsorbent prepared from agricultural solid waste for the adsorption and desorption of cationic dye. *Emergent Materials*, 5(6), 1767–1780. https://doi.org/10.1007/s42247-022-00390-y
- Aljeboree, A. M., Alkaim, A. F. and Al-Dwody, M. A. (2022). Modification of low-cost adsorbent prepared from agricultural solid waste for the adsorption and desorption of cationic dye. *Emergent Materials*, 5(6), 1767–1780. https://doi.org/10.1007/s42247-022-00390-y
- Andriambahiny, R.N.A., Das, J., Roy, B. *et al.* (2025). A review on the recent advancement of acid modified bio-adsorbents for the removal of methyl orange dye from wastewater treatment. *Discover Chemistry*, 2, 92. https://doi.org/10.1007/s44371-025-00180-5
- Bouchouirbat, I., Rghioui, L. and Najih, R. (2022). Optimization based on response surface methodology of anionic dye desorption from two agricultural solid wastes. *Chemistry Africa*, 5(4), 1127–1138. https://doi.org/10.1007/s42250-022-00395-4
- Bouziani, A., Boudrahem, F. and Bouazizi, N. (2024). Efficient adsorption removal of an anionic azo dye by lignocellulosic waste material and sludge recycling into combustible briquettes. *Processes*, *12*(2), 352. https://doi.org/10.3390/pr12020352
- El Haddad, M., Slimani, R., Mamouni, R. and El Antri, S. (2022). Modification of low-cost adsorbent prepared from agricultural solid waste for the adsorption and desorption of cationic dye. *Emergent Materials*, *5*(6), 1563–1575. https://doi.org/10.1007/s42247-022-00390-y
- El Haddad, M., Slimani, R., Mamouni, R. and El Antri, S. (2022). Modification of low-cost adsorbent prepared from agricultural solid waste for the adsorption and desorption of cationic dye. *Emergent Materials*, *5*(6), 1563–1575. https://doi.org/10.1007/s42247-022-00390-y
- El-Hafed S., Miyah Y., Benjelloun M., Souhassou H., Nahali L., Boualam O., Kherbeche A., Zerrouq F., Bouslamti R., Agunaou M. (2024) Optimization of CWPO for the Crystal violet and Methyl orange dyes degradation in the presence of copper-impregnated Moroccan clay catalysts, *Mor. J. Chem.*, 12(3), 1097-1109
- El Mrabet, R., Rghioui, L., Zegaoui, O. and Moussout, H. (2024). Evaluation of almond shell activated carbon for dye (methylene blue and malachite green) removal by experimental and simulation studies. *Materials*, 17(24), 6077. https://doi.org/10.3390/ma17246077

- El Ouahabi, I., Moussout, H. and Boukhlifi, F. (2022). Study of the adsorption properties of an almond shell in the elimination of methylene blue in an aquatic medium. *Moroccan Journal of Chemistry*, 10(3), 543–552. https://revues.imist.ma/index.php/morjchem/article/view/33140
- El Ouahabi, I., Moussout, H. and Boukhlifi, F. (2022). Study of the adsorption properties of an almond shell in the elimination of methylene blue in an aquatic medium. *Moroccan Journal of Chemistry*, 10(3), 543–552. https://www.mdpi.com/1996-1944/17/24/6077
- Elmansouri, I., Benali, O. and Saadi, S. (2024). Synthesis of water hyacinth stem (WHS)-based bioadsorbent for the removal of methylene blue (MB) and congo red (CR) dyes from synthetic wastewater. ResearchGate. https://www.researchgate.net/publication/314653310
- Farch, S., Houdaifa, H. and Akretche, D. E. (2024). Comparative study of almond shell raw activated carbon, chemically activated and adsorption of anionic dye from wastewater. In *Proceedings of the 7th International Conference on Materials and Environmental Science (ICMES)* (pp. 305–313). AIJR Books. https://books.aijr.org/index.php/press/catalog/book/170/chapter/3221
- Gharbi, S. and Bouchdoug, M. (2021). Removal of cationic dye from aqueous solution using agricultural wastes: Argan and almond shells. *Iranica Journal of Energy and Environment,* 12(2), 128–135. https://doi.org/10.5829/ijee.2021.12.02.08
- Husaini M. (2021). Corrosion inhibition effect of benzaldehyde (methoxybenzene) for aluminium in sulphuric acid solution, *Alger. J. Eng. Technol.*, 4, 74–80. https://aljet.com/index.php/aljet
- Husaini M. (2024). Role of organic compound as corrosion inhibitor for aluminium in acidic solution, *Arab. J. Chem. Environ. Res.*, 11(2), 95–109. https://www.mocedes.org/ajcer/
- Husaini M., Danladi Y., Hamza M. (2025a). Utilization of activated carbon produced from agricultural waste for Congo red adsorption, *Afr. J. Manag. Eng. Technol.*, 3(6), 166–176. https://revues.imist.ma/index.php/AJMET/article/view/59357
- Husaini M., Danladi Y., Hamza M. (2025b). Preparation and characterization of activated carbon from almond seed shell found in the Federal Polytechnic Idah Metropolis, *J. Mater. Environ. Sci.*, 16(9), 1609–1621. https://jmaterenvironsci.com/Document/vol16/vol16_N9/JMES-2025-1609092-Husaini.pdf
- Husaini M., Danladi Y., Hamza M. (2025c). Wastewater remediation by adsorption using activated carbon prepared from almond residues collected at the Federal Polytechnic Idah premises, *Arab. J. Chem. Environ. Res.*, 12(2), 110–123. https://www.mocedes.org/ajcer/
- Husaini M., Hamza M., Ibrahim Z., Ibrahim J. (2025d). Investigation of the inhibition effect of benzaldehyde on the corrosion of aluminium in nitric acid solution, *J. Mater. Environ. Sci.*, 16(5), 754–767. https://jmaterenvironsci.com/Document/vol16/vol16_N5/JMES-2025-1605052-Husaini.pdf
- Husaini M., Ibrahim M.B. (2025). Adsorption of cationic and anionic dyes in single and binary systems onto activated carbon derived from agricultural waste, *J. Mater. Environ. Sci.*, 16(5), 881–893. https://jmaterenvironsci.com/Document/vol16/vol16_N5/JMES-2025-1605061-Husaini.pdf
- Husaini M., Usman B., Ibrahim M.B. (2023a). Thermodynamic and equilibrium evaluation for anionic dye adsorption using utilized biomass-based activated carbon: regeneration and reusability studies, *Arab. J. Chem. Environ. Res.*, 10(1), 1–16.
- Husaini M., Usman B., Ibrahim M.B. (2023b). Combined computational and experimental studies for the removal of anionic dyes using activated carbon derived from agricultural waste, *Appl. J. Environ. Eng. Sci.*, 9(4), 245–258. https://revues.imist.ma/index.php/AJEES

- Husaini M., Usman B., Ibrahim M.B. (2023c). Competitive adsorption of Congo red dye from aqueous solution onto activated carbon derived from black plum seed shell in single and multicomponent system, *Afr. J. Manag. Eng. Technol.*, 1(2), 76–89. https://revues.imist.ma/index.php/AJMET/article/view/59357
- Husaini M., Usman B., Ibrahim M.B. (2023d). Kinetic and thermodynamic evaluation on removal of anionic dye from aqueous solution using activated carbon derived from agricultural waste: equilibrium and reusability studies, *Appl. J. Environ. Eng. Sci.*, 9, 124–138. https://revues.imist.ma/index.php/AJEES/article/view/40418
- Husaini M., Usman B., Ibrahim M.B. (2023e). Modeling and equilibrium studies for the adsorption of Congo red using *Detarium microcarpum* seed shell activated carbon, *Appl. J. Environ. Eng. Sci.*, 9, 147–162. https://revues.imist.ma/index.php/AJEES/article/view/40602
- Husaini M., Usman B., Ibrahim M.B. (2023f). Adsorption studies of methylene blue using activated carbon derived from sweet detar seed shell, *ChemSearch J.*, 14(1), 21–32. https://www.researchgate.net/publication/372411212
- Husaini M., Usman B., Ibrahim M.B. (2024a). Biosorption of methyl orange dye in single, binary and ternary systems onto gingerbread plum seed shell activated carbon, *J. Turk. Chem. Soc. Sec. A*, 11(2), 655–664. https://doi.org/10.18596/jotcsa.1372995
- Husaini M., Usman B., Ibrahim M.B. (2024b). Experimental and quantum chemical evaluation for methylene blue adsorption onto activated carbon, *Afr. J. Manag. Eng. Technol.*, 2(1), 51–62. https://revues.imist.ma/index.php/AJMET/article/view/50278
- Jodeh S., Hamed O., Melhem A., Salghi R., Jodeh D., Azzaoui K., et al. (2018). Magnetic nanocellulose from olive industry solid waste for the effective removal of methylene blue from wastewater, *Environmental Science and Pollution Research*, 25 (22), 22060-22074
- Khalfaoui, M. and Abdennouri, M. (2021). Adsorption of crystal violet dye from aqueous solutions onto low-cost untreated and NaOH treated almond shell. *Iranian Journal of Chemistry and Chemical Engineering*, 40(5), 1305–1318. https://doi.org/10.30492/IJCCE.2021.51269
- Latifi S., Saoiabi S., Alanazi M. M., Boukra O., Krime A., El Hammari L., *et al.* (2025), Low-Cost Titania-Hydroxyapatite (TiHAp) nanocomposites were synthesized for removal of Methylene blue under Solar and UV irradiation, *Next Materials*, 8, 100859, ISSN 2949-8228, https://doi.org/10.1016/j.nxmate.2025.100859
- Martínez-Casillas, D. C., García-Reyes, R. B. and Salazar-Rabago, J. J. (2024). Almond and walnut shell activated carbon for methylene blue adsorption. *ACS Sustainable Resource Management*, 2(2), 211–220. https://doi.org/10.1021/acssusresmgt.4c00080
- Mbarek, M., Jedli, H., Rabhi, R. and Slimi, K. (2024). Activated carbon derived from olive waste for the adsorption of methylene blue and methyl orange dyes. *ChemistrySelect*, *9*(46), e202404066. https://doi.org/10.1002/slct.202404066
- Mbarek, N., Kchaou, M., Khiari, B. and Jeguirim, M. (2024). Sustainable removal of cationic and anionic dyes using activated carbons derived from agricultural residues: A comparative study. *Environmental Research*, 252, 118891. https://doi.org/10.1016/j.envres.2024.118891
- N'diaye A.D., Hammouti B., Nandiyanto A.B.D., Al Husaeni D. F. (2022), A review of biomaterial as an adsorbent: From the bibliometric literature review, the definition of dyes and adsorbent, the adsorption phenomena and isotherm models, factors affecting the adsorption process, to the use of Typha species waste as a low-cost adsorbent, *Communications in Science and Technology*, 7 No.1, 140-153

- Ollo K., Aliou Guillaume P. L., Franck K. K., Berté M., Quand-même G. C. and Ouattara L. (2022). Behavior of boron-doped diamond anode on methyl orange oxidation, *J. Mater. Environ. Sci.*, 13(11), 1264-1277
- Othmani, M., Amami, S. (2024). Adsorption behavior of methylene blue onto activated coconut shells: Kinetic, thermodynamic, mechanism and regeneration of the adsorbent. *Journal of Nanomaterials and Molecular Nanotechnology*, 19(2), 45–57. https://doi.org/10.1177/15593258241290708
- Rajendran, J., Panneerselvam, A., Ramasamy, S. and Palanisamy, P. (2024). Methylene blue and methyl orange removal from wastewater by magnetic adsorbent based on activated carbon synthesised from watermelon shell. *Desalination and Water Treatment*, 317, 100040. https://doi.org/10.1016/j.dwt.2024.100040
- Rajendran, R., Vigneshwaran, S., Subramaniam, R. (2024). Valorization of agricultural by-products for wastewater treatment: Surface modification and adsorption performance. *Journal of Environmental Chemical Engineering*, 12(5), 113247. https://doi.org/10.1016/j.jece.2024.113247
- Ranjbar, A. and Ghasemi, F. (2025). A review on the recent advancement of acid modified bio-adsorbents for the removal of methyl orange dye from wastewater treatment. *Environmental Chemistry for a Sustainable World*, 5(1), 33–55. https://doi.org/10.1007/s44371-025-00180-5
- Sahu, O., and Gupta, R. (2024). Almond and walnut shell activated carbon for methylene blue adsorption. *ACS Sustainable Resource Management*, 3(2), 185–194. https://doi.org/10.1021/acssusresmgt.4c00080
- Salazar-Rabago, J. J., García-Reyes, R. B., Ríos-Badrán, I. M. and Ramírez-Serrano, J. L. (2024). Evaluation of almond shell activated carbon for dye (methylene blue and malachite green) removal by experimental and simulation studies. *Materials*, *17*(24), 6077. https://doi.org/10.3390/ma17246077
- Sukmana, H., Radojčin, M., Gyulavári, T., Kozma, G., Kónya, Z. and Hodúr, C. (2025). Utilization of rice husks as effective bioadsorbents for methylene blue removal from wastewater: Characterization, adsorption performance and regeneration studies. *Applied Water Science*, *15*, 148. https://doi.org/10.1007/s13201-025-02511-4
- Tabaght F.E., Azzaoui K., Elidrissi A., Hamed O., Mejdoubi E., Jodeh S., *et al.* (2021). New nanostructure based on hydroxyapatite modified cellulose for bone substitute, synthesis, and characterization *International Journal of Polymeric Materials and Polymeric Biomaterials*, 70(6), 437-448
- Zerrouk M., Er-rajy M., Azzaoui K., Sabbahi R., Hanbali G., Jodeh S., Alshahateet S.F., Hammouti B., Kaya S., Maslov M. M., Lachkar M., Ouarsal R. (2025), DFT Computation-Assisted Design and synthesis of trisodium nickel triphosphate: Crystal Structure, Vibrational study, DFT Computation, Electronic Properties and Application in Wastewater Purification, *Journal of Molecular Structure*, 141450, ISSN 0022-2860, https://doi.org/10.1016/j.molstruc.2025.141450